

Developed ARL by Integral Equation Solutions to Monitor Changes under Autocorrelated Data for the DEWMA Chart

Yupaporn Areepong and Kotchaporn Karoon

Abstract—The DEWMA control chart was developed as a useful tool to monitor the process mean quickly under autocorrelated data. The Average Run Length (ARL) metric, which is designed for control charts, is intended for measuring the ability of the control chart. In this work, an analytical Integral Equation or explicit ARL will be developed for data on the DEWMA control chart that are characterized by a quadratic trend AR(1) model. Banach's fixed point theorem was used to prove its uniqueness and existence after it was generated by the second form of the Fredholm integral equation. It has evolved compared to the ARL obtained via the Numerical Integral Equation (numerical IE) approach and looked at in connection with the EWMA chart, which has shown to have superior detection capabilities. The AEQL and RMI metrics were used to confirm their ability. Furthermore, real-world data from the relevant domains of finance and economics was used to test this suggested technique.

Index Terms—Integral equation solution, average run length, Banach's fixed point, DEWMA control chart.

I. INTRODUCTION

CONTROL chart is the instruments available in the statistical process control (SPC) discipline for tracking and identifying changes in the process mean. The Shewhart control chart is often used to detect significant changes [1]. There are two types of control charts for identifying tiny changes: cumulative sum (CUSUM) [2] and exponentially weighted moving average (EWMA) [3]. Control chart details are available in Montgomery [4]. Next, extensive literature has noted that many control charts were developed from EWMA-type control charts. They exceeded the standard EWMA control chart in terms of sensitivity in monitoring tiny changes in the process. For example, the modified exponentially weighted moving average (MEWMA) chart [5] enables monitoring of tiny changes. After Shamma and Shamma presented the control chart, which is the double exponentially weighted moving average (DEWMA) [6], Mahmoud and Woodall adjusted it [7]. This control chart is useful for rapidly identifying little changes.

Small amounts of the autocorrelation between subsequent observations can significantly impact the control chart's statistical characteristics. Several researchers have examined

how autocorrelation affects control chart efficiency. Specifically, autocorrelation levels generated during or moving average MA(1) or autoregressive AR(1) time series models were slightly or significantly raised, which made it more difficult to identify out-of-control alerts on the CUSUM chart seen in Johnson and Bagshaw [8]). Nonetheless, the autocorrelated data might be the result of the other control chart, such as EWMA, and a modification of the EWMA type. Time series observations have become prevalent in the real world. In particular, trends and seasonality, together with an AR or MA component [9], [10], can potentially be integrated into a time series model via data from the financial and economic domains.

To maximize accuracy, it is best to reduce "white noise," or the discrepancy between estimated and real values. Despite usually having a normal distribution, the autocorrelated data can also produce white noise, also known as Gaussian white noise. However, non-Gaussian white noise has an intriguing exponential distribution and may be used to express a wide range of data. In their earlier work, Mohamed and Hocine focused specifically on white noise in their Bayesian research on AR(1) with exponential white noise [11]. Suparman [12] suggested estimating parameters for an AR model under exponential white noise.

A common metric used to assess the success rate of a control chart is the ARL or average run length. A control chart's performance could be represented as the average number of observations required to identify an out-of-control state in the process multiplied by the probable probability of detecting an out-of-control signal. The average number of observations a process in control makes before indicating that it is out of control is known as ARL_0 . On the other hand, the average number of observations, also known as ARL_1 , is necessary to detect an out-of-control change in a process variable. The ARL_0 value should be large. Conversely, the ARL_1 number has to be as low as feasible to show that the procedure is suitable for quickly identifying any out-of-control circumstances.

There are several methods that have been proposed for computing the ARL of a control chart, involving the integral equation (IE), the Markov Chain method, and Monte Carlo simulation. However, this study discusses the IE approach, which is often used for computing ARL. There are two options in the IE approach: numerical IE and analytical IE. The numerical IE was converted into a system of linear equations using the Fredholm integral equation of the second type, and its existence and uniqueness were verified using Banach's fixed point theorem. In contrast, the analytical IE was built using explicit formulas. Hawkins [13] utilized IE

Manuscript received March 14, 2024; revised June 13, 2024. This work was supported in part by Naresuan University under Grant R2567C013.

Y. Areepong is a Professor of Applied Statistics Department, King Mongkut's University of Technology North Bangkok, Bangkok, 10800 Thailand, (e-mail:yupaporn.a@sci.kmutnb.ac.th).

K. Karoon is a lecturer of Mathematics Department and Research Center for Academic Excellence in Mathematics, Naresuan University, Phitsanulok, 65000 Thailand, (corresponding author to provide e-mail:kotchapornt@nu.ac.th).

to calculate the ARL of the CUSUM chart, whereas Crowder [14] utilized IE to evaluate the ARL of the EWMA chart. Vanbrackle and Reynolds [15] devised the ARL using the Markov Chain approach and analytical IE with the EWMA and CUSUM charts, which were based on the first-order autoregressive AR(1) model. Phanyaem [16] created explicit formulas for IE on the CUSUM chart, which were originally run under the SARMA model. Karoon et al. presented explicit formulas for underlying trend AR(p) and seasonal AR(p) processes on the extended EWMA control chart using the IE technique and applied them to real-world data in various fields [17],[18]. Phanthuna et al. [19] developed the exact ARL of the modified EWMA control chart using IE methods and compared its performance to traditional control charts under the AR(1) model. In addition, Karoon and Areepong [20],[21] improved the ARL of the DEWMA chart using IE methods and compared the abilities of other control charts, both simulated and real-world data, based on the obtained seasonal AR(p) and trend AR(p) model. Recently, Phanthuna et al. [22] presented the ARL with the IE approach of a double modified EWMA (DMEWMA) chart under AR model.

Based on the literature reviews above, the analytical IE of ARL was validated for its existence and uniqueness before deriving an explicit ARL solution. Furthermore, it is necessary to demonstrate both the existence and uniqueness of explicit ARL equations using Banach's fixed point theorem. The purpose of this work was to create an ARL for detecting changes in the first-order quadratic trend autoregressive (AR(1)) process with exponential white noise. It was run on the DEWMA control chart, utilizing analytical and numerical IE methods. Furthermore, it was not previously discovered for evaluating ARL using a quadratic trend AR model. At last, this explicit ARL was applied to real-world data, and it is discussed in this study in terms of finance and economics.

II. PRELIMINARIES

This section examines the fundamentals of the first-order quadratic trend autoregressive process, often known as the quadratic trend AR(1) process, and its underlying exponential white noise. Additionally, the ARL formula that was created utilizing analytical and numerical IE techniques displayed the statistical structure of the DEWMA control chart. And then, the final subsection covers Banach's fixed-point theorem.

A. The First-Order Quadratic Trend Autoregressive Process

The quadratic trend AR(1) process, or the first-order quadratic trend, was generalized from the Box-Jenkins ARIMA model. Time series are widely used in many domains, including technology, epidemiology, finance, and economics. Let X_t be a sequence from a quadratic trend AR(1) model defined as

$$X_t = \eta + \omega t + \rho t^2 + \phi_1 X_{t-1} + \xi_t \quad (1)$$

where η is the constant of the process, the ω and ρ are coefficients corresponding to time t and t^2 , respectively. The error terms, as given in $\xi_t \sim Exp(\alpha)$, are expected to be exponentially distributed white noise. The initial coefficient of the autoregressive process is ϕ_1 with $0 < \phi_1 \leq 1$.

B. Fundamentals of the Structure of the Control Charts

The EWMA control chart is an instrument utilized in SPC to monitor and identify minor to moderate deviations in the process mean. The recursive equation below could possibly have been used to state the EWMA control chart [3] statistic.

$$E_t = \lambda X_t + (1 - \lambda)E_{t-1}, t = 1, 2, 3, \dots, \quad (2)$$

where EWMA control chart parameter X_t represent a sequence of the quadratic trend AR(1) process with running based on exponential white noise. λ denotes an exponential smoothing parameter with $0 < \lambda \leq 1$. In this work, the variance of EWMA statistic (E_t) is

$$(1 - (1 - \lambda)^{2t}) \left(\frac{\lambda}{2 - \lambda} \right) \sigma^2.$$

If t gets large, the term consists of t converge to 0. X_t is a process with mean (μ) and variance (σ^2). The upper (UCL) and lower (LCL) control limits for detecting process changes are as follows:

$$UCL = \mu + G\sigma\sqrt{\frac{\lambda}{2 - \lambda}},$$

$$LCL = \mu - G\sigma\sqrt{\frac{\lambda}{2 - \lambda}},$$

where G is the width of control limit of EWMA control chart. And then, the stopping time (E_t) can be expressed as

$$\tau_b = inf \{ t \geq 0 : E_t > b \},$$

where b is the upper control limit (UCL) of EWMA control chart.

The DEWMA control chart, developed by Mahmoud and Woodall [6] in 2010, is a valuable substitute method for detecting minute modifications in the process. The DEWMA control chart statistic can be shown using the following equation:

$$E_t = \lambda_2 X_t + (1 - \lambda_2)E_{t-1},$$

$$W_t = \lambda_1 E_t + (1 - \lambda_1)W_{t-1}, t = 1, 2, 3, \dots, \quad (3)$$

where λ_1 and λ_2 are the exponential smoothing parameters of DEWMA chart under $0 < \lambda_1, \lambda_2 \leq 1$. X_t is a process with mean (μ) and variance (σ^2). The variance of W_t is

$$\sigma^2 \frac{\lambda_1^2 \lambda_2^2}{(\lambda_1 - \lambda_2)^2} (A + B - 2C).$$

where A , B , and C represent

$$\frac{(1 - (1 - \lambda_2)^{2t})(1 - \lambda_2)^2}{1 - (1 - \lambda_2)^2},$$

$$\frac{(1 - (1 - \lambda_1)^{2t})(1 - \lambda_1)^2}{1 - (1 - \lambda_1)^2},$$

$$\frac{(1 - ((1 - \lambda_1)(1 - \lambda_2))^t)(1 - \lambda_1)(1 - \lambda_2)}{1 - (1 - \lambda_1)(1 - \lambda_2)},$$

respectively.

If t gets large, the term that exists of t converges to 0. From the DEWMA control chart, the following are the upper

(UCL) and lower (LCL) control limits for identifying process changes:

$$UCL = \mu + \hat{G}\sigma U,$$

$$LCL = \mu - \hat{G}\sigma U,$$

where U represents

$$\sqrt{\frac{\lambda_1^2 \lambda_2^2}{(\lambda_1 - \lambda_2)^2} (A + B - 2C)},$$

and \hat{G} is expressed as the width of control limit of DEWMA control chart. And then, the stopping time (W_t) can be expressed as

$$\tau_h = \inf \{t \geq 0 : W_t > h\},$$

where h is the upper control limit (UCL) of DEWMA control chart. When $\lambda_1 = 1$ in (3), the DEWMA statistic transforms into the EWMA statistic, see in (2).

C. Feature of the ARL

In the whole project, the error term (ξ_t) is a series of continuous, i.i.d. random variables drawn from the exponential distribution or denoted as ($f(x, \alpha)$). The following is an expression for the ARL feature:

$$ARL = \begin{cases} ARL_0 = E_\infty(\tau_h), \theta = \infty \\ ARL_1 = E_1(\tau_h), \theta = 1 \end{cases}.$$

Here, the change point was considered as follows:

$$\xi_t = \begin{cases} Exp(\alpha_0), t = 1, 2, \dots, \theta - 1 \\ Exp(\alpha_1), t = \theta, \theta + 1, \dots \end{cases},$$

where $E_\theta()$ is the expectation under ($\xi_t \sim Exp(\alpha)$), α_0 and α_1 are known parameters. Herein, $\theta = \infty$ denotes no change in the process, also called the in-control process of ARL (ARL_0). While $\theta = 1$ denotes the first time of change from α_0 to α_1 in the process, we refer to it as an out-of-control process of ARL (ARL_1).

D. Analytical IE for the ARL on the DEWMA Control Chart with Quadratic Trend AR(1) process

The ARL for the Fredholm integral equation of the second kind was built in this section utilizing analytical IE[23]. The approximate ARL on the DEWMA control chart is used to track modifications in the quadratic trend AR (1). To begin, substitute (1) into (3) as shown below:

$$W_t = \lambda_1 \lambda_2 (\eta + \omega t + \varrho t^2 + \phi_1 X_{t-1} + \xi_t) + \lambda_2 (1 - \lambda_1) E_{t-1} + (1 - \lambda_2) W_{t-1}.$$

Since $t = 1$ for the first time, the initial values $E_0 = \varepsilon$ and $W_0 = \nu$ are established. The DEWMA statistic with quadratic trend AR(1) can be stated as follows:

$$W_t = \lambda_1 \lambda_2 (D + \xi_1) + \lambda_2 (1 - \lambda_1) \varepsilon + (1 - \lambda_2) \nu.$$

where D denotes $\eta + \omega + \varrho + \phi_1 X_0$.

In the control process, W_1 can be written as bound control limits between l and h as:

$$l < W_1 < h.$$

The variable ξ_1 can be expressed as the interval of the control limit as follows:

$$l - \lambda_2 (\lambda_1 D + z_1) - z_2 < \xi_1 \lambda_1 \lambda_2 < h - \lambda_2 (\lambda_1 D + z_1) - z_2$$

then,

$$\frac{l - z_2}{\lambda_1 \lambda_2} - \frac{(\lambda_1 D + z_1)}{\lambda_1} < \xi_1 < \frac{h - z_2}{\lambda_1 \lambda_2} - \frac{(\lambda_1 D + z_1)}{\lambda_1},$$

where z_1 and z_2 are $(1 - \lambda_1)\varepsilon$ and $(1 - \lambda_2)\nu$, respectively.

Theorem 1: The Fredholm integral equation of the second kind is applied to solve the analytical IE ARL on the DEWMA chart.

Considering the function below, it represents the Fredholm integral equation of the second sort.

$$\varphi(\nu) = 1 + \int_{\frac{l - z_2}{\lambda_1 \lambda_2} - \frac{(\lambda_1 D + z_1)}{\lambda_1}}^{\frac{h - z_2}{\lambda_1 \lambda_2} - \frac{(\lambda_1 D + z_1)}{\lambda_1}} \varphi(W_1) f(\xi_1) d\xi_1.$$

Proof: Let $\varphi(\nu)$ represents the analytical IE ARL that corresponds to the quadratic trend AR(1) process on the DEWMA chart. Also,

Let

$$\psi = \lambda_1 \lambda_2 D + \lambda_2 z_1 + z_2 + \lambda_1 \lambda_2 \xi_1$$

ψ was rewritten in term of ξ_1 as follows:

$$\xi_1 = \frac{\psi - \lambda_1 \lambda_2 D - \lambda_2 z_1 - z_2}{\lambda_1 \lambda_2}$$

$$= \frac{\psi - z_2}{\lambda_1 \lambda_2} - \frac{(\lambda_1 D + z_1)}{\lambda_1}$$

will get

$$d\xi_1 = \frac{1}{\lambda_1 \lambda_2} d\psi.$$

Therefore, the equation rearranged is

$$\varphi(\nu) = 1 + \frac{1}{\lambda_1 \lambda_2} \int_l^h \varphi(\psi) f(\xi_1) d\psi.$$

By changing the integral variable, it will be the equation in (4) below.

$$\varphi(\nu) = 1 + \frac{1}{\lambda_1 \lambda_2} \int_l^h \varphi(\psi) f\left(\frac{\psi - z_2}{\lambda_1 \lambda_2} - \frac{(\lambda_1 D + z_1)}{\lambda_1}\right) d\psi. \tag{4}$$

In this study, ξ_1 is defined as an exponential distribution with parameter α . Therefore, the Fredholm integral equation of the second sort for analytical ARL can be presented as:

$$\varphi(\nu) = 1 + \frac{Q(\psi)}{\alpha \lambda_1 \lambda_2} Y, \tag{5}$$

where

$$Q(\psi) = e^{\frac{z_2}{\lambda_1 \lambda_2} - \frac{(\lambda_1 D + z_1)}{\lambda_1}},$$

$$Y = \int_l^h \varphi(\psi) e^{\frac{-\psi}{\alpha \lambda_1 \lambda_2}} d\psi,$$

and

$$\Omega_0(\psi) = e^{\frac{-\psi}{\alpha \lambda_1 \lambda_2}}.$$

In this paper, we considered the interval control limit $[o, h]$. So, l is determined as 0. After (5) was proved by Banach's fixed point theorem, which will be shown in the

last subsection, the result showed proportional existence and uniqueness.

The integral equation Y , which can be rewritten as:

$$\begin{aligned}
 Y &= \frac{1}{\alpha\lambda_1\lambda_2} \int_0^h [1 + Q(\psi)Y] e^{\frac{-\psi}{\alpha\lambda_1\lambda_2}} d\psi \\
 &= -\alpha\lambda_1\lambda_2[\Omega_0(h)-1] + \frac{Y}{\alpha\lambda_1\lambda_2} e^{\frac{z_2}{\alpha\lambda_1\lambda_2} - \frac{(\lambda_1 D + z_1)}{\alpha\lambda_1}} \int_0^h e^{\frac{-\psi}{\alpha\lambda_1}} d\psi \\
 &= -\alpha\lambda_1\lambda_2[\Omega_0(h) - 1] - \frac{Y}{\lambda_2} e^{\frac{z_2}{\alpha\lambda_1\lambda_2} - \frac{(\lambda_1 D + z_1)}{\alpha\lambda_1}} [\Omega_0(h\lambda_2) - 1]
 \end{aligned}$$

Thus, it can be rearranged as

$$Y = \frac{-\alpha\lambda_1\lambda_2[\Omega_0(h) - 1]}{1 + \frac{e^{\frac{z_2}{\alpha\lambda_1\lambda_2} - \frac{(\lambda_1 D + z_1)}{\alpha\lambda_1}}}{\lambda_2} [\Omega_0(h\lambda_2) - 1]}$$

Finally, the equation (5) is substituted into the integral equation Y . By constructing the Fredholm integral equation of the second sort, the analytical ARL of the DEWMA chart can possibly be derived as follows:

$$\varphi(\nu) = 1 - \frac{\lambda_2\Omega(z_2) [\Omega_0(h) - 1]}{\lambda_2\Omega_0(-\lambda_2(\lambda_1 D + z_1)) + [\Omega_0(h\lambda_2) - 1]} \quad (6)$$

The proof of analytic ARL or explicit formulas for ARL is complete. ■

In (6), the in-control ARL, or ARL_0 , is represented by substituting α with α_0 . Similarly, the out-of-control ARL (ARL_1) is illustrated by substituting α with α_1 . Then, $\alpha_1 = \alpha_0(1 + \delta)$, and δ represented the shift changes in the monitoring process.

E. Numerical IE for the ARL on the DEWMA Control Chart with Quadratic Trend AR(1) Process

This study employs the Gauss-Legendre quadrature rules methodology to implement an approximation ARL based on the numerical IE method.

Definition 1: The quadratic rules commonly used for the integral equation

$$\int_0^h f(s)ds$$

can also be estimated by the sum of the areas of a rectangle, as follows:

$$\int_0^h W(s)f(s)ds \approx \sum_{j=1}^m w_j f(c_j),$$

where $c_j = \frac{h}{m} (j - \frac{1}{2})$, $j = 1, 2, \dots, m$, the integral f value is defined by utilizing base h/m with heights at the interval midpoints rule, and $W(s)$ is weight function. The interval $[0, h]$ is divided into $0 \leq c_1 \leq c_2 \leq \dots \leq c_m \leq h$, and set of constant weights $w_j = h/m$; $j = 1, 2, \dots, m$.

Theorem 2: The numerical IE method $\vartheta(\nu)$ under quadratic trend AR(1) with exponential white noise on the DEWMA chart could be shown in (7) as:

$$\vartheta(\nu) = 1 + \frac{1}{\lambda_1\lambda_2} \sum_{j=1}^m w_j \vartheta(c_j) f\left(\frac{c_j - z_2}{\lambda_1\lambda_2} - \frac{(\lambda_1 D + z_1)}{\lambda_1}\right), \quad (7)$$

where $z_2 = (1 - \lambda_2)\nu$ and $j = 1, 2, \dots, m$.

Proof: The Gauss-Legendre quadrature procedure was used to apply the $\vartheta(\nu)$ to the estimated ARL from the integral equation in (4). Substituting ν with c_j in (7), and it was rearranged as yields equation (8), that is:

$$\vartheta(c_i) = 1 + \frac{1}{\lambda_1\lambda_2} \sum_{j=1}^m w_j \vartheta(c_j) f\left(\frac{c_j - c_i}{\lambda_1\lambda_2} - \frac{z_1 - c_i}{\lambda_1} - D\right), \quad (8)$$

where $i = 1, 2, \dots, m$.

Solving the system in terms of m linear equation, the equation (8) can be rearranged to look like this:

$$\begin{aligned}
 \vartheta(c_1) &= 1 + \frac{1}{\lambda_1\lambda_2} \sum_{j=1}^m w_j \vartheta(c_j) f\left(\frac{c_j - c_1}{\lambda_1\lambda_2} - \frac{z_1 - c_1}{\lambda_1} - D\right) \\
 \vartheta(c_2) &= 1 + \frac{1}{\lambda_1\lambda_2} \sum_{j=1}^m w_j \vartheta(c_j) f\left(\frac{c_j - c_2}{\lambda_1\lambda_2} - \frac{z_1 - c_2}{\lambda_1} - D\right) \\
 &\vdots \\
 \vartheta(c_m) &= 1 + \frac{1}{\lambda_1\lambda_2} \sum_{j=1}^m w_j \vartheta(c_j) f\left(\frac{c_j - c_m}{\lambda_1\lambda_2} - \frac{z_1 - c_m}{\lambda_1} - D\right)
 \end{aligned}$$

This is identical to the matrix form

$L_{m \times 1} = 1_{m \times 1} + R_{m \times m} L_{m \times 1}$ and $(I_m - R_{m \times m})^{-1}$ exists. The unique solution that can be written is

$$L_{m \times 1} = (I_m - R_{m \times m})^{-1} 1_{m \times 1}, \text{ where } L_{m \times 1} = \begin{bmatrix} \vartheta(c_1) \\ \vdots \\ \vartheta(c_m) \end{bmatrix},$$

$$1_{m \times 1} = \begin{bmatrix} 1 \\ \vdots \\ 1 \end{bmatrix}, I_m = \text{diag}(1, 1, \dots, 1) \text{ is a identity matrix,}$$

and $R_{m \times m}$ is a matrix of $(m, m)^{th}$ elements:

$$R_{m \times m} = \frac{1}{\lambda_1\lambda_2} \begin{bmatrix} r_{11} & r_{12} & \cdots & r_{1m} \\ r_{21} & r_{22} & \cdots & r_{2m} \\ \vdots & \vdots & \ddots & \vdots \\ r_{m1} & r_{m2} & \cdots & r_{mm} \end{bmatrix}$$

where

$$r_{ij} = w_j f\left(\frac{c_j - c_i}{\lambda_1\lambda_2} - \frac{z_1 - c_i}{\lambda_1} - D\right) : i, j = 1, 2, \dots, m. \quad \blacksquare$$

The approximation for the integral equation can be derived from the summation where c_j is substituted by ν in $\vartheta(c_j)$, completing the proof.

F. The uniqueness and existence of ARL's analytical IE Running on DEWMA Chart

The second-kind Fredholm integral equation is influenced by the analytical IE for the ARL of the DEWMA control chart with the quadratic trend AR(1) process. The uniqueness and existence of the ARL solution are shown in this section using Banach's fixed-point theorem.

Definition 2: A fixed point that represents a mapping $T : X \rightarrow X$ of a set X across itself represents a mapping from $x \in X$ onto itself, that is

$$Tx = x.$$

Definition 3: Let a metric space be represented by (X, d) . A contraction on X is defined as a mapping $T : X \rightarrow X$, provided that there is a positive constant $K < 1$ such that

$$d(T(x), T(y)) \leq Kd(x, y); \forall x, y \in X$$

In terms of geometry, this suggests that the images $T(x)$ and $T(y)$ exhibit a closer relationship than the points x and y .

Theorem 3: Banach’s Fixed Point Theorem

Let $T : X \rightarrow X$ represent a contraction mapping with contraction constant $0 \leq u < 1$. Let (X, d) represent a full metric space.

Then

$$\|T(\varphi(\nu)_1) - T(\varphi(\nu)_2)\| \leq u \|\varphi(\nu)_1 - \varphi(\nu)_2\|,$$

for all $\varphi(\nu)_1, \varphi(\nu)_2 \in X$. has to show a unique fixed point $x \in X$ (such that $T(\varphi(\nu)) = \varphi(\nu)$), i.e. a unique fixed-point in X [23].

Proof: To present that T in (9) represents mapping of contraction for $\varphi(\nu)_1, \varphi(\nu)_2 \in [0, h]$ by show that

$$\|T(\varphi(\nu)_1) - T(\varphi(\nu)_2)\| \leq u \|\varphi(\nu)_1 - \varphi(\nu)_2\|,$$

for all

$$\varphi(\nu)_1, \varphi(\nu)_2 \in u[0, h]$$

with $0 \leq u < 1$ under the norm

$$\|\varphi(\nu)\|_\infty = \sup_{\nu \in [0, h]} |\varphi(\nu)|.$$

From (5), consider T as an operation in the (9) class of all continuous functions, and also substitute 0 for l , as the following example illustrates.

$$T(\varphi(\nu)) = 1 + \frac{1}{\alpha\lambda_1\lambda_2} e^{\frac{(1-\lambda_2)\nu}{\lambda_1\lambda_2} - \frac{(\lambda_1 D + z_1)}{\lambda_1}} \int_0^h \varphi(\psi)\Omega_0(\psi) d\psi. \tag{9}$$

Consider: $\|T(\varphi(\nu)_1) - T(\varphi(\nu)_2)\|_\infty$

$$= \sup_{\nu \in [0, h]} \left| \frac{Q(\psi)}{\alpha\lambda_1\lambda_2} \int_0^h (\varphi_1(\psi) - \varphi_2(\psi)\Omega_0(\psi)) d\psi \right|$$

$$\leq \sup_{\nu \in [0, h]} \|T(\varphi(\nu)_1) - T(\varphi(\nu)_2)\|_\infty Q(\psi) (\Omega_0(h) - 1)$$

$$= \|T(\varphi(\nu)_1) - T(\varphi(\nu)_2)\|_\infty \sup_{\nu \in [0, h]} |Q(\psi)| |\Omega_0(h) - 1|$$

$$\leq u \|T(\varphi(\nu)_1) - T(\varphi(\nu)_2)\|_\infty,$$

where

$$u = \sup_{\nu \in [0, h]} |Q(\psi)| \left| e^{\frac{-h}{\alpha\lambda_1\lambda_2}} - 1 \right|; 0 \leq u < 1.$$

The explicit formula for ARL, or the analytical IE for ARL, is the existence and uniqueness of a solution that can be solved wholly with the help of Banach’s fixed-point theorem.

III. THE EFFICACY EVALUATION FOR CONTROL CHART

The efficacy of a control chart is often measured in terms of ARL. In the article, the analytical IE for ARL (denoted as $\varphi(\nu)$) was compared to the numerical IE for ARL (denoted as $\vartheta(\nu)$) using the absolute percentage relative change (%APRC), which was computed using the equation (10) below [24].

$$\%APRC = \left| \frac{\varphi(\nu) - \vartheta(\nu)}{\varphi(\nu)} \right| \times 100\% \tag{10}$$

Next, the efficacy of ARL was evaluated using the average extra quadratic loss, which is called AEQL, and the relative mean index, or refer to RMI matrices [25]. These were operated under various parameters and various control charts.

One of these, the AEQL, is derived by applying it across a variety of shift sizes, which can then be assessed using overall performance metrics. The AEQL is computed in (11) below:

$$AEQL = \frac{1}{\Theta} \sum_{\delta_i = \delta_{min}}^{\delta_{min}} (\delta_i^2 \times ARL(\delta_i)) \tag{11}$$

where δ_i represents the value of shift change order i , $ARL(\delta_i)$ is explicit ARL value of each control chart for the value of shift change order i , and Θ represents the total amounts of shift change order i from δ_{min} to δ_{max} .

Another one is the RMI, which is used to calculate each control chart’s efficacy via the mathematical formula in (12) as

$$RMI = \frac{1}{n} \sum_{i=1}^n \left(\frac{ARL_i - \min ARL_i}{\min ARL_i} \right) \tag{12}$$

where ARL_i denotes the ARL of control chart that calculated using the shift size in terms of row i , and $\min ARL_i$ represents the lowest ARL of overall control charts compared to the shift size in terms of row i , for $i = 1, 2, \dots, n$.

The control chart with the highest efficacy for identifying process changes under quadratic trend AR(1) with exponential white noise is the one with the lowest AEQL and RMI values.

IV. EXPERIMENTAL RESULTS

Here, the simulation studies on the DEWMA control chart compare the efficacy of the analytical IE or explicit formula $\varphi(\nu)$ with the numerical IE or NIE approach $\vartheta(\nu)$ for the quadratic trend AR(1) process. The efficacy of the ARL of both methods was initially evaluated by determining that $\delta = 0$ is an in-control process and $\delta > 0$ is an out-of-control process. The numerical IE for ARL is generated with the amount of division points or denotes $m = 500$. In this research, the MATHEMATICA mathematical software was used to calculate the analytical and numerical IEs for ARL. The results were obtained using an Intel(R) Core(TM) i5-8250U CPU and 4.00 GB RAM.

The state of the calculated ARL can be described as follows:

Input:

- 1) Define in-control process at $ARL_0 = 370$
- 2) Set parameters such as the coefficient of the quadratic trend AR(1) model, including ϕ_1, η, ω , and ϱ
- 3) Set the lower control limit (LCL), herein it is $l = 0$
- 4) Set the control chart parameters, including λ_2 equal to 0.05 and 0.10, and then $\lambda_1 = 0.4\lambda_2$, $\lambda_1 = \lambda_2$, and $\lambda_1 = 1$ represent DEWMA with unequal λ , DEWMA with equal λ , and EWMA, respectively.
- 5) Set parameters for two states of the control process under the error term ($\xi_t \sim Exp(\alpha)$), namely α instead of α_0 for the in-control (ARL_0), whereas α instead of $\alpha_1 = (1 + \delta)\alpha_0$ for the out-of-control (ARL_1)
- 6) Set shift changes in the process or showed as δ equals 0.0001, 0.0005, 0.001, 0.005, 0.01, 0.05, 0.1, 0.2, 0.5

Output:

- 1) Find the upper control limit (h) from calculating and determining ARL_0 equals 370
- 2) Compute the ARL_1 for each shift size by using the upper control (h) value obtained by the previous step and varying the values of the shift size δ .

The results in Tables I and II show the results of comparing the ARL_1 values with varying shift changes running on the DEWMA chart for the quadratic trend AR(1) process based on determining parameters λ as two conditions, namely cases of equal λ (refer to $\lambda_1 = \lambda_2$) and cases of unequal λ (refer to $\lambda_1 = 0.4\lambda_2$). They were compared in percentage of %APRC and calculation time in seconds. The results show that the ARL_1 values of both techniques show hardly any difference, but the ARL for the analytical IE method expresses superior efficacy in terms of computation time, which shows that it appears very instantly in all situations. On the other hand, the ARL for the numerical IE method expresses the computation time slower than the analytical IE method in approximately three seconds for all shift changes in all situations.

Note that "time" in the whole table in this research is to show the computational time of the ARL that was obtained by the numerical IE method, whereas the computational time of the ARL that was obtained by the analytical IE method has very little value, or approximately 0.001 seconds, so it is not displayed in the table.

V. ILLUSTRATIVE EXAMPLE OF REAL-WORLD DATA

This section presents the results of implementing the suggested the analytical IE and numerical IE techniques to monitor changes on the DEWMA control chart using real data, which is running under the quadratic trend AR(1) process with exponential white noise. The real data consists of a monthly natural gas futures price dataset in USD, covering the period from January 2018 to February 2024, with 74 observations. The real-world dataset was fitted to the quadratic trend AR(1) model. The whole parameters was estimated using the statistical software package SPSS. The results in Table III indicates that the the dataset is suitable for quadratic trend AR(1) model presenting statistically significant parameters with coefficients $\phi_1 = 0.877, \omega = 0.182, \varrho = -0.002$. The Kolmogorov-Simirov test was used to determine if the residual series of a white noise distribution was asymptotic or exponential. The findings demonstrate that

the white noise strongly fitted the exponential distribution at a P-value of $0.366 > 0.05$ and a mean equal to 0.7166 while the process under control, as stated in Table IV.

Furthermore, the model's appropriateness has been verified by plotting a line graph between the real and fitted dataset components, which appear to be in almost identical agreement, as illustrated in Fig. 1. According to the previously stated text, the quadratic trend AR(1) model X_t could possibly be expressed mathematically as follows:

$$X_t = 0.182t - 0.002t^2 + 0.877X_{t-1} + \xi_t,$$

where

$$\xi_t \sim Exp(\alpha_0 = 0.7166).$$

Next, ARL_1 was used to calculate the analytical IE and the numerical IE under various parameters after computing the control limits for $ARL_0 = 370$ using (6) and vary used under small shift sizes ($0 < \delta < 0.05$) and moderate shift sizes ($0.05 < \delta < 0.50$). The capabilities of the two techniques are expressed in Table V and VI. The ARL_1 findings from both methodologies were identical to those in Table I and II, which shows simulated data. However, the computing time for the analytical IE approach was practically instantaneous, which is significantly lower than that of the numerical IE technique. So, this indicates that the analytical IE for ARL_1 is an effective way to detect changes in the process on the DEWMA control chart.

After that, the quadratic trend AR(1) process using real data was applied to both the EWMA and DEWMA charts. The control charts' efficiency was compared in terms of ARL_1 , which is derived from analytical IE and fluctuates with shift changes ranging from small to moderate in the process mean. For the efficiency comparison, the smoothing parameter λ of the EWMA chart was defined as $\lambda = \lambda_2$ equal to 0.05, 0.10, and providing $\lambda_1 = 1$ of the DEWMA chart became the EWMA chart. The comparative findings are given in Table VII. The DEWMA chart provided a smaller ARL_1 than the EWMA chart in all cases. The DEWMA chart that is defined as $\lambda_1 = 0.4\lambda_2$ provided the smallest ARL_1 when compared to the DEWMA control chart that determined $\lambda_1 = \lambda_2$ and the EWMA control chart, illustrated as Figs. 2 and 3. Moreover, the efficiencies of the DEWMA control chart were confirmed by computing metrics such as the RMI and AEQL values, which were calculated by formulas in (11) and (12), respectively. Both metrics provided the lowest value for the DEWMA control chart with unequal λ under the coefficients, which were determined as $\lambda_1 < \lambda_2$ and subordinate as the DEWMA control chart with equal λ , and the biggest value for the EWMA control chart, as shown in Table VIII and Fig. 4. It is noted that the bold in Table VIII express the lowest values of RMI and AEQL when comparing whole values between the whole control chart in this study. As a result, control charts showing the lowest RMI and AEQL values are better tracked and detected than other control charts. The RMI and AEQL values also show results that correspond to the out-of-control ARL or ARL_1 values.

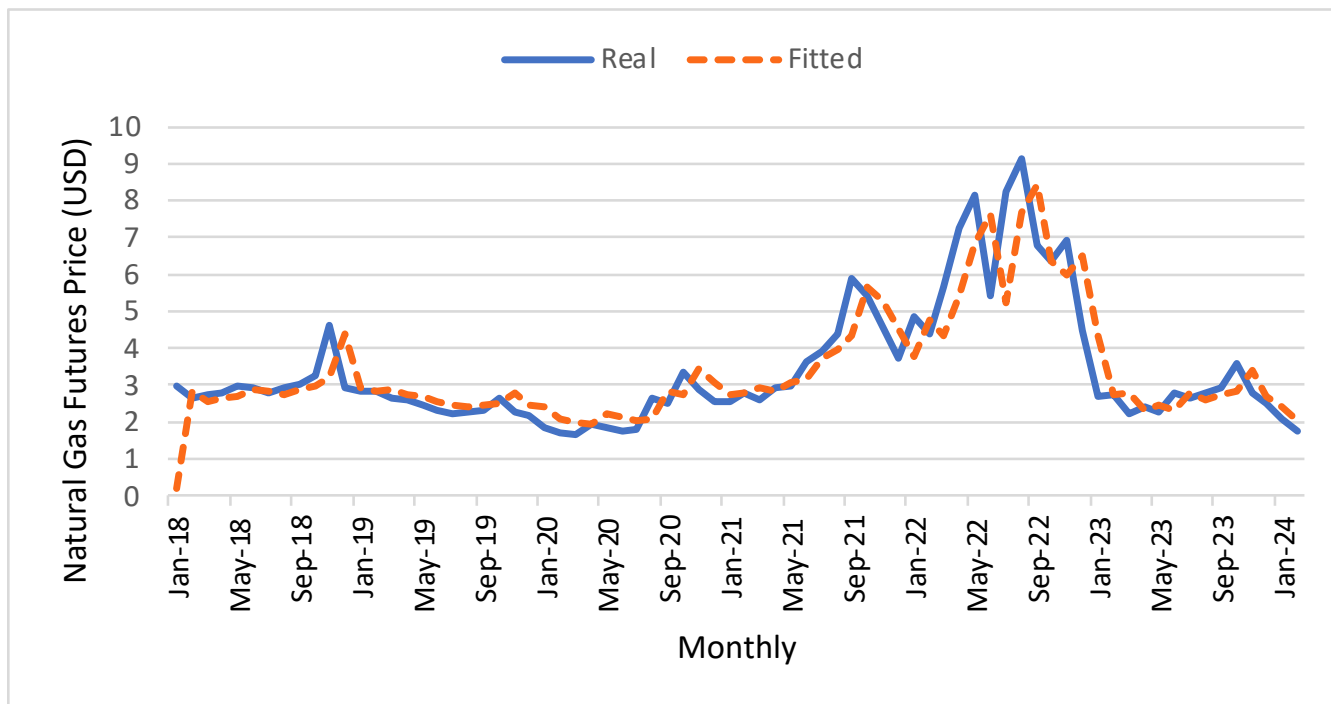


Fig. 1. The monthly dataset of natural gas futures price was showed real-data and fitted model under the quadratic trend AR(1) model

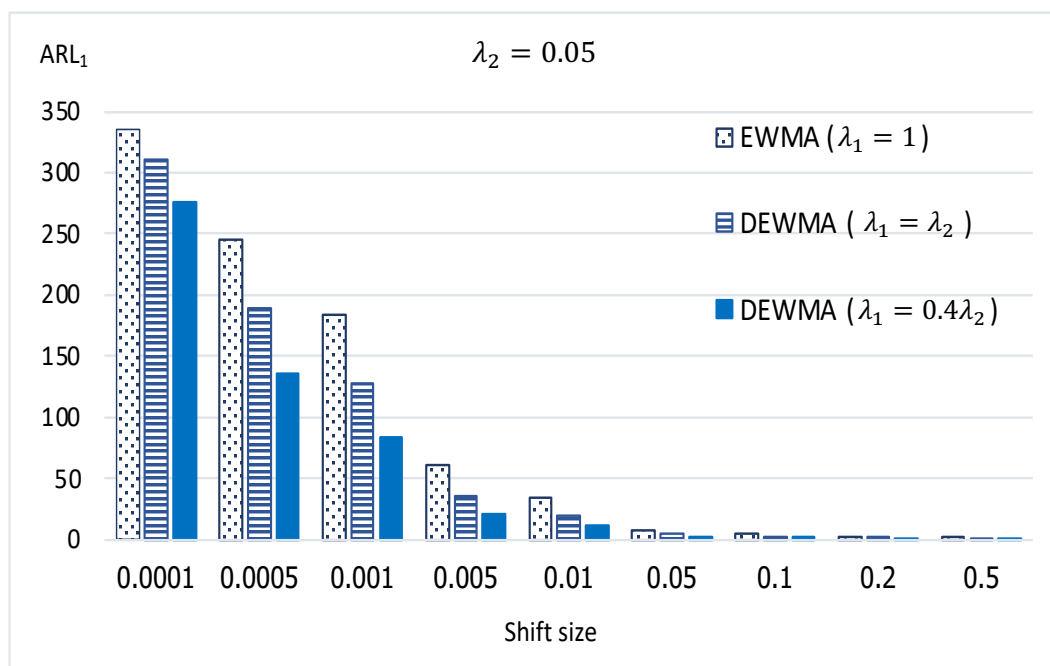


Fig. 2. ARL_1 values of the control charts with the datasets of natural gas futures under the quadratic trend AR(1) process with $\lambda_2 = 0.05$ for $ARL_0 = 370$

This means that, under these conditions, the DEWMA control chart outperformed the EWMA control chart, particularly when specified as $\lambda_1 < \lambda_2$, which in cases of this study expressed $\lambda_1 = 0.4\lambda_2$.

After that, we had to demonstrate the performance of the DEWMA control chart when used to detect shift changes in the process with real-life data. In Figs. 5 and 6, we express the detecting performance of the DEWMA chart when compared to the EWMA chart. In this part, the smoothing parameters ($\lambda_2 = 0.05$ and $\lambda_1 = 0.4\lambda_2$) were determined for the DEWMA chart, which is compared to

the EWMA chart with $\lambda = \lambda_2 = 0.05$ in terms of detecting changes. The first detection signal was issued at the 11th and 56th observation points on the DEWMA and EWMA control charts, respectively (the observations in red are plotted above the UCL, which shows a green line). These findings support the effectiveness of the suggested analytical IE for ARL on the DEWMA chart. This has a direct impact on the price of natural gas futures, and checking out changes is important in both the economy and finance. From the viewpoint of investors, the control chart above can be applied to the starting point for making lucrative investment decisions.

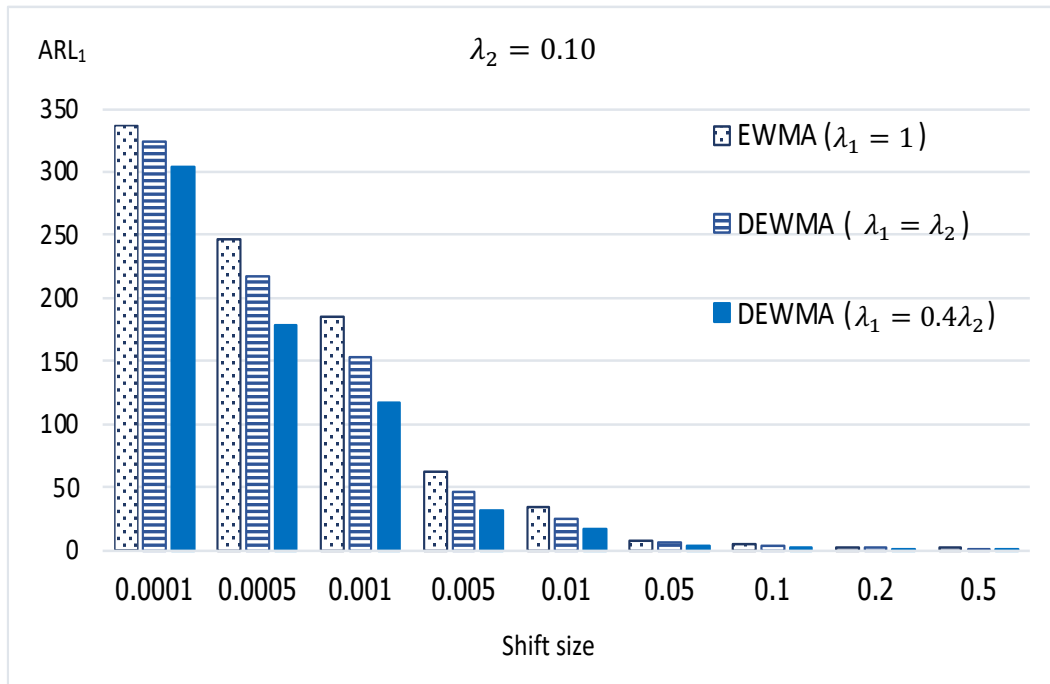


Fig. 3. ARL_1 values of the control charts with the datasets of natural gas futures under the quadratic trend AR(1) process with $\lambda_2 = 0.10$ for $ARL_0 = 370$

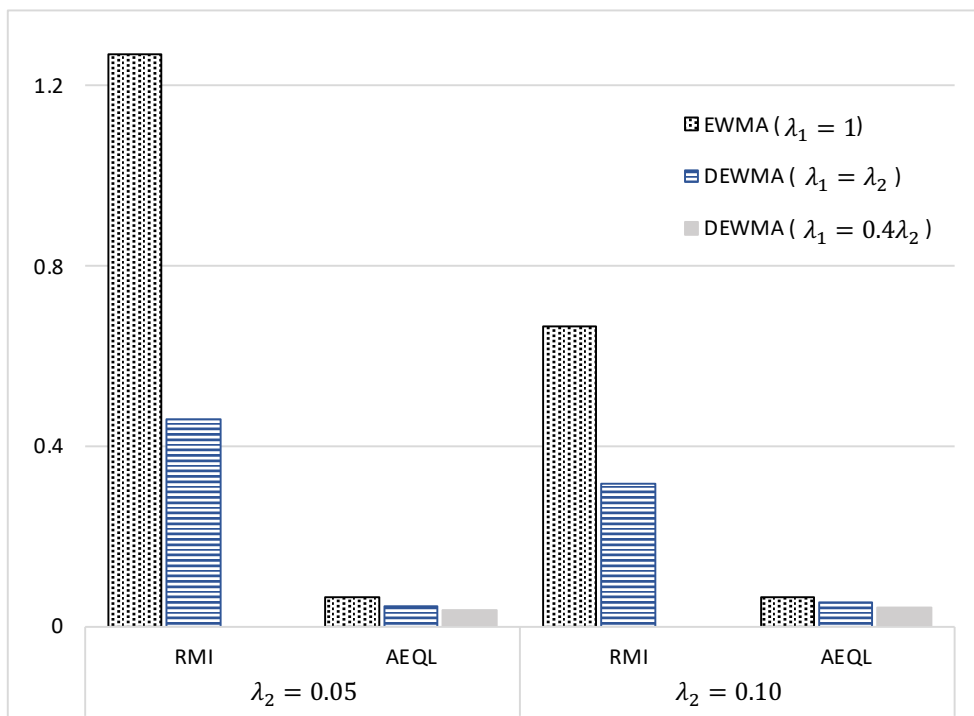


Fig. 4. RMI and AEQL values for evaluating efficiency of the control charts with the datasets of natural gas futures price under the quadratic trend AR(1) with $\lambda_2 = 0.05$ and $\lambda_2 = 0.10$

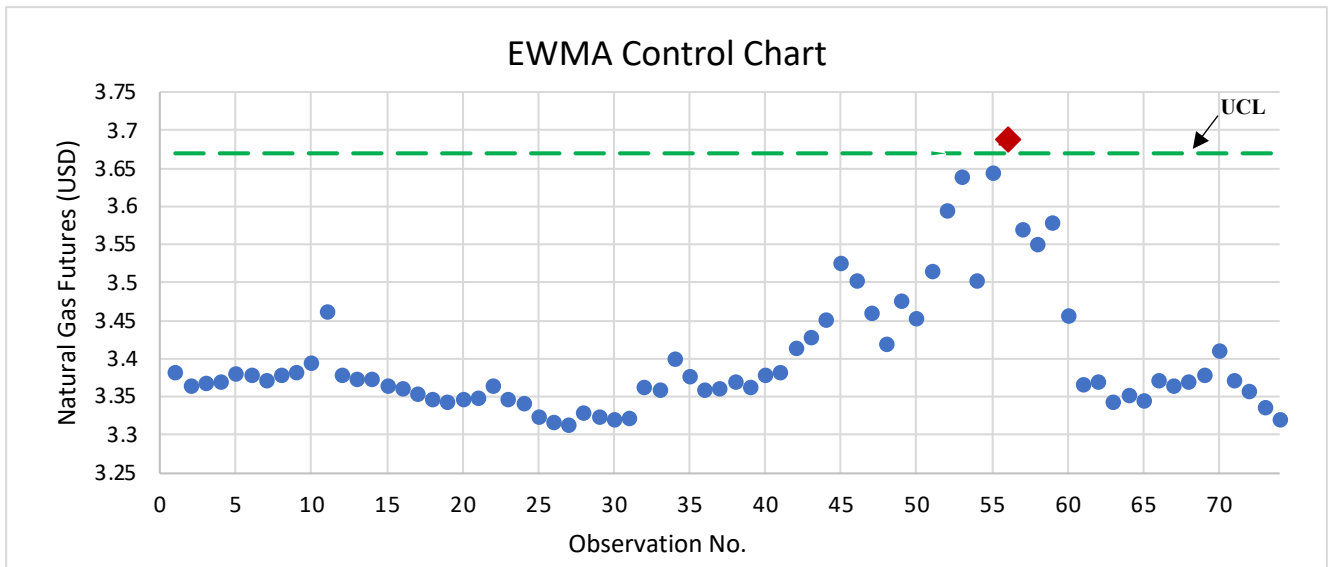


Fig. 5. Detecting changes for quadratic trend AR(1) process for the datasets of natural gas futures running on EWMA control chart with $\lambda_1 = 1$

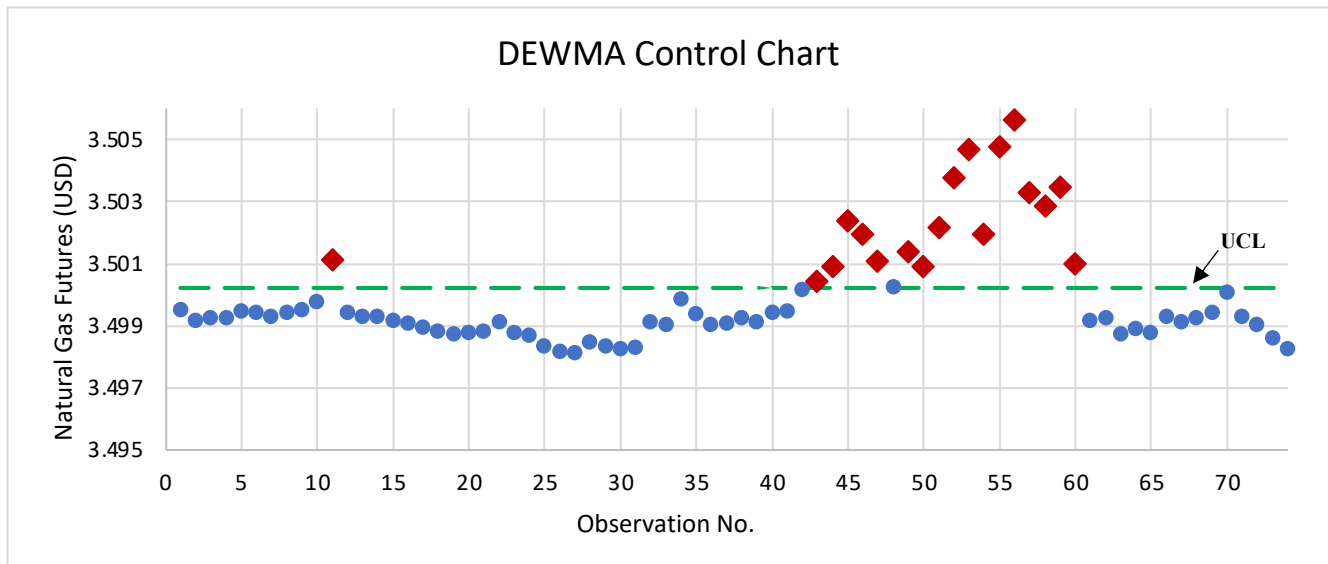


Fig. 6. Detecting changes for quadratic trend AR(1) process for the datasets of natural gas futures running on DEWMA control chart with $\lambda_1 = 0.4\lambda_2$

VI. CONCLUSIONS

By analyzing and evaluating the ARL computation, analytical and numerical IE approaches can be utilized to determine the effectiveness of a control chart. In the current study, the quadratic trend AR(1) process with exponential white noise was tracked using both techniques for determining the ARL on the DEWMA chart. By comparing calculation times and employing the absolute percentage relative change benchmark, the computation of ARL was utilized to confirm the accuracy of the analytical ARL, also referred to as explicit ARL. Compared to numerical ARL, which requires substantially longer computation times, analytical ARL performs better and can be calculated instantly. The suggested ARL, which operates on the DEWMA chart, can be expanded to compare to the EWMA chart. It shows more capability detecting than the EWMA chart for all studies under the condition's study. So, the DEWMA chart is an excellent option for identifying tiny and moderate shift changes in both simulated and real

data under autocorrelated data, particularly when specified as $\lambda_1 < \lambda_2$. And then, the fitted model is the quadratic trend AR(1) model, similar to the reviews of literature in the first section, such as [20], [21]. However, determining the appropriate values of the DEWMA control chart in these scenarios might be difficult. As a consequence, determining the most appropriate values for the parameters of the DEWMA control chart should be researched further. The study's scope might be expanded to include various types of procedures for actual data with varying features.

REFERENCES

- [1] W.A. Shewhart, "Quality Control Charts," *Bell System Technical Journal*, vol. 2, pp. 593-603, 1926.
- [2] E.S. Page, "Continuous Inspection Schemes," *Biometrika*, vol. 41, no. 1-2, pp. 100-115, 1954.
- [3] W.S. Roberts, "Control Chart Tests based on Geometric Moving Averages," *Technometrics*, vol. 1, no. 3, pp. 239-250, 1959.
- [4] D.C. Montgomery, *Introduction to Statistical Quality Control*, 6th ed., John Wiley and Sons, New York, 2009.

TABLE I

COMPARING ARL_1 OBTAINED BY THE ANALYTICAL AND NUMERICAL IE TECHNIQUES OF THE DEWMA CHART UNDER QUADRATIC TREND AR(1) PROCESS FOR $ARL_0 = 370$ WITH $\eta = 1, \omega = 0.3, \rho = 0.5, \lambda_1 = \lambda_2$, AND $\lambda_2 = 0.05$

δ	ϕ_1	0.2	-0.2
	h	0.000050495	0.0000753491
0.0001	$\varphi(\nu)$	313.301115208	316.749204596
	$\vartheta(\nu)$	313.301115172	316.749204512
	time	2.749	2.875
	%APRC	1.169E-08	2.651E-08
0.0005	$\varphi(\nu)$	193.759037054	201.040395570
	$\vartheta(\nu)$	193.759037035	201.040395526
	time	3.015	2.953
	%APRC	9.816E-09	2.215E-08
0.001	$\varphi(\nu)$	131.318612119	138.142914506
	$\vartheta(\nu)$	131.318612106	138.142914478
	time	2.937	2.922
	%APRC	9.635E-09	2.029E-08
0.005	$\varphi(\nu)$	37.1051635088	39.8438802849
	$\vartheta(\nu)$	37.1051635061	39.8438802786
	time	2.938	2.890
	%APRC	7.187E-09	1.594E-08
0.01	$\varphi(\nu)$	19.8423547644	21.3717437523
	$\vartheta(\nu)$	19.8423547631	21.3717437491
	time	2.874	2.891
	%APRC	6.649E-09	1.495E-08
0.05	$\varphi(\nu)$	4.70243308278	5.04802587954
	$\vartheta(\nu)$	4.70243308255	5.04802587898
	time	2.859	2.953
	%APRC	4.897E-09	1.112E-08
0.1	$\varphi(\nu)$	2.73243894931	2.91289706242
	$\vartheta(\nu)$	2.73243894922	2.91289706217
	time	2.907	2.938
	%APRC	3.572E-09	8.257E-09
0.2	$\varphi(\nu)$	1.76041426731	1.85490762548
	$\vartheta(\nu)$	1.76041426727	1.85490762539
	time	2.921	2.984
	%APRC	2.044E-09	4.856E-09
0.5	$\varphi(\nu)$	1.21993867069	1.25871817298
	$\vartheta(\nu)$	1.21993867068	1.25871817296
	time	2.954	3.079
	%APRC	5.459E-10	1.384E-09

TABLE II

COMPARING ARL_1 OBTAINED BY THE ANALYTICAL AND NUMERICAL IE TECHNIQUES OF THE DEWMA CHART UNDER QUADRATIC TREND AR(1) PROCESS FOR $ARL_0 = 370$ WITH $\eta = 1, \omega = 0.3, \rho = -0.5, \lambda_1 = 0.4\lambda_2$, AND $\lambda_2 = 0.10$

δ	ϕ_1	0.4	-0.4
	h	0.000109152	0.00024334
0.0001	$\varphi(\nu)$	315.889777618	323.832324169
	$\vartheta(\nu)$	315.889777454	323.832323309
	time	2.906	2.844
	%APRC	5.206E-08	2.657E-07
0.0005	$\varphi(\nu)$	199.240725216	215.440208438
	$\vartheta(\nu)$	199.240725142	215.440208015
	time	3.016	2.984
	%APRC	3.720E-08	1.963E-07
0.001	$\varphi(\nu)$	136.443960371	152.006719469
	$\vartheta(\nu)$	136.443960332	152.006719232
	time	3.015	2.952
	%APRC	2.904E-08	1.560E-07
0.005	$\varphi(\nu)$	39.1525099033	45.7143936031
	$\vartheta(\nu)$	39.1525098968	45.7143935633
	time	2.968	3.001
	%APRC	1.659E-08	8.718E-08
0.01	$\varphi(\nu)$	20.9843982909	24.6865939244
	$\vartheta(\nu)$	20.9843982880	24.6865939066
	time	2.875	2.968
	%APRC	1.395E-08	7.214E-08
0.05	$\varphi(\nu)$	4.95988722533	5.80596282070
	$\vartheta(\nu)$	4.95988722487	5.80596281788
	time	3.000	2.970
	%APRC	9.353E-09	4.859E-08
0.1	$\varphi(\nu)$	2.86662958919	3.31058262434
	$\vartheta(\nu)$	2.86662958900	3.31058262314
	time	2.938	2.921
	%APRC	6.802E-09	3.642E-08
0.2	$\varphi(\nu)$	1.83047591840	2.06524855418
	$\vartheta(\nu)$	1.83047591833	2.06524855372
	time	2.921	3.077
	%APRC	3.943E-09	2.233E-08
0.5	$\varphi(\nu)$	1.24850986344	1.34814254776
	$\vartheta(\nu)$	1.24850986342	1.34814254766
	time	2.907	2.999
	%APRC	1.101E-09	7.105E-09

TABLE III

THE QUADRATIC TREND AR(1) COEFFICIENTS FOR THE DATASET OF NATURAL GAS FUTURES PRICE FROM JANUARY 2018 TO FEBRUARY 2024

Variable	Coefficient	Std. Error	t	Sig.
AR(1) (ϕ_1)	0.877	0.055	15.832	0.000
ω	0.182	0.062	2.956	0.004
ρ	-0.002	0.001	-2.028	0.046

[5] N. Khan, M. Aslam and C.H. Jun, "Design of a Control Chart using a Modified EWMA Statistic," *Quality and Reliability Engineering International*, vol. 33, no. 5, pp. 1095-1104, 2017.

[6] S.E. Shamma and A.K. Shamma, "Development and Evaluation of Control Charts using Double Exponentially Weighted Moving Averages," *International Journal of Quality and Reliability Management*, vol. 9, no. 6, pp. 18-25, 1992.

[7] A.A. Mahmoud and W.H. Woodall, "An Evaluation of the Double Exponentially Weighted Moving Average Control Chart," *Communications in Statistics - Simulation and Computation*, vol. 39, no. 5, pp. 933-949, 2010.

[8] M. Bagshaw and R.A. Johnson, "The Effect of Serial Correlation on the Performance of CUSUM Tests II," *Technometrics*, vol. 17, no. 1, pp. 73-80, 1975.

[9] L. Xu and W. Chen, "Construction and Simulation of Economic

TABLE IV

TESTING THE SUITABILITY OF EXPONENTIAL WHITE NOISE USING THE KOLMOGOROV-SMIRNOV TEST

α_0	Kolmogorov-Smirnov Z	Sig.
0.7166	0.920	0.366

TABLE V

COMPARING ARL_1 OBTAINED BY THE ANALYTICAL AND NUMERICAL IE TECHNIQUES WITH NATURAL GAS FUTURES DATASETS ON DEWMA CHART AND FITTED MODEL AS A QUADRATIC TREND AR(1) WITH $\eta = 0, \omega = 0.182, \rho = -0.002, \phi_1 = 0.877$ AND $\lambda_1 = \lambda_2$

δ	λ_1	$\lambda_1 = \lambda_2$	
	λ_2 h	0.05 0.0000288496	0.10 0.000467211
0.0001	$\varphi(\nu)$	310.901613026	324.150749630
	$\vartheta(\nu)$	310.901613005	324.150748639
	time	2.922	3.062
	%APRC	6.741E-09	3.058E-07
0.0005	$\varphi(\nu)$	189.659149414	216.766540925
	$\vartheta(\nu)$	189.659149404	216.766540433
	time	2.718	2.892
	%APRC	5.329E-09	2.269E-07
0.001	$\varphi(\nu)$	127.636993174	153.405301968
	$\vartheta(\nu)$	127.636993167	153.405301691
	time	2.938	3.031
	%APRC	5.176E-09	1.805E-07
0.005	$\varphi(\nu)$	35.6990496113	46.3658120666
	$\vartheta(\nu)$	35.6990496097	46.3658120199
	time	3.000	2.922
	%APRC	4.502E-09	1.007E-07
0.01	$\varphi(\nu)$	19.0635634790	25.0601229655
	$\vartheta(\nu)$	19.0635634782	25.0601229446
	time	2.875	2.999
	%APRC	4.235E-09	8.318E-08
0.05	$\varphi(\nu)$	4.52791571863	5.89271333767
	$\vartheta(\nu)$	4.52791571849	5.89271333437
	time	2.906	2.953
	%APRC	3.088E-09	5.604E-08
0.1	$\varphi(\nu)$	2.64160786349	3.35634366506
	$\vartheta(\nu)$	2.64160786343	3.35634366365
	time	3.000	3.032
	%APRC	2.224E-09	4.210E-08
0.2	$\varphi(\nu)$	1.71316014403	2.08966421554
	$\vartheta(\nu)$	1.71316014401	2.08966421499
	time	2.859	2.985
	%APRC	1.249E-09	2.594E-08
0.5	$\varphi(\nu)$	1.20096916623	1.35878369486
	$\vartheta(\nu)$	1.20096916623	1.35878369475
	time	2.969	2.968
	%APRC	3.222E-10	8.344E-09

TABLE VI

COMPARING ARL_1 OBTAINED BY THE ANALYTICAL AND NUMERICAL IE TECHNIQUES WITH NATURAL GAS FUTURES DATASETS ON DEWMA CHART AND FITTED MODEL AS A QUADRATIC TREND AR(1) WITH $\eta = 0, \omega = 0.182, \rho = -0.002, \phi_1 = 0.877$ AND $\lambda_1 = 0.4\lambda_2$

δ	λ_1	$\lambda_1 = 0.4\lambda_2$	
	λ_2 h	0.05 0.000000175337	0.10 0.0000229736
0.0001	$\varphi(\nu)$	275.628385856	304.303642943
	$\vartheta(\nu)$	275.628385773	304.303642931
	time	3.173	2.875
	%APRC	3.012E-08	3.911E-09
0.0005	$\varphi(\nu)$	136.404693741	178.177387947
	$\vartheta(\nu)$	136.404693763	178.177387941
	time	2.921	2.984
	%APRC	1.593E-08	3.214E-09
0.001	$\varphi(\nu)$	83.7753961133	117.507762330
	$\vartheta(\nu)$	83.7753961091	117.507762328
	time	2.985	2.907
	%APRC	5.067E-09	1.810E-09
0.005	$\varphi(\nu)$	20.8899339504	31.9532604611
	$\vartheta(\nu)$	20.8899339496	31.9532604606
	time	2.906	2.985
	%APRC	3.896E-09	1.484E-09
0.01	$\varphi(\nu)$	11.0376255677	17.0019633053
	$\vartheta(\nu)$	11.0376255674	17.0019633051
	time	3.016	3.000
	%APRC	2.167E-09	1.156E-09
0.05	$\varphi(\nu)$	2.77237634817	4.06915151876
	$\vartheta(\nu)$	2.77237634816	4.06915151873
	time	2.968	2.968
	%APRC	3.127E-10	7.709E-10
0.1	$\varphi(\nu)$	1.74154967709	2.40371243003
	$\vartheta(\nu)$	1.74154967709	2.40371243002
	time	3.063	2.876
	%APRC	1.205E-11	5.296E-10
0.2	$\varphi(\nu)$	1.26250664800	1.59046811212
	$\vartheta(\nu)$	1.26250664800	1.59046811212
	time	2.938	2.969
	%APRC	2.139E-11	2.785E-10
0.5	$\varphi(\nu)$	1.04342648279	1.15326761212
	$\vartheta(\nu)$	1.04342648279	1.15326761212
	time	2.937	2.953
	%APRC	9.576E-13	6.331E-11

Statistics Measurement Model based on Time Series Analysis and Forecast," *Complexity*, Article ID 5963516, 9 pages, 2021.

[10] S.K. Klutse, "Inflation Forecasting in Developing Economies Using SARMA Models: The Case of Ghana," in *Proc. the European Union's Contention in the Reshaping Global Economy*, pp. 286-302, 2021.

[11] I. Mohamed and F. Hocine, "Bayesian Estimation of an AR(1) Process with Exponential White Noise," *Journal of Theoretical and Applied Sciences*, vol. 37, pp. 365-372, 2003.

[12] S. Suparman, "A New Estimation Procedure Using a Reversible Jump MCMC Algorithm for AR Models of Exponential White Noise," *International Journal of GEOMATE*, vol. 15, no. 49, pp. 85-91, 2018.

[13] D.M. Hawkins, "A CUSUM for a Scale Parameter," *Journal of Quality Technology*, vol. 13, no. 4, pp. 228-231, 1981.

TABLE VII

COMPARISON OF ARL_1 OBTAINED BY ANALYTICAL IE TECHNIQUE WITH THE DATASETS OF NATURAL GAS FUTURES RUNNING ON THE EWMA AND DEWMA CHARTS AND FITTED MODEL AS THE QUADRATIC TREND $AR(1)$ WITH PARAMETERS: $\eta = 0, \omega = 0.182, \rho = -0.002, \phi_1 = 0.877$ FOR $ARL_0 = 370$

λ_2	δ	Control chart		
		EWMA $\lambda_1 = 1$	DEWMA $\lambda_1 = \lambda_2$	DEWMA $\lambda_1 = 0.4\lambda_2$
0.05 ¹	0.0001	335.997	310.902	275.628
	0.0005	245.680	189.659	136.405
	0.001	183.992	127.637	83.775
	0.005	61.595	35.699	20.890
	0.01	33.958	19.064	11.038
	0.05	8.010	4.528	2.772
	0.1	4.486	2.642	1.742
	0.2	2.704	1.713	1.263
	0.5	1.640	1.201	1.043
0.10 ²	0.0001	336.895	324.151	304.304
	0.0005	246.653	216.767	178.177
	0.001	184.882	153.405	117.508
	0.005	61.996	46.366	31.953
	0.01	34.188	25.060	17.002
	0.05	8.061	5.893	4.069
	0.1	4.511	3.356	2.404
	0.2	2.716	2.090	1.590
	0.5	1.645	1.359	1.153

¹ $b = 0.00822407, h = 0.0000288496, \text{and } h = 0.000000175337$ for $\lambda_1 = 1, \lambda_2,$ and $0.4\lambda_2$
² $b = 0.0165435, h = 0.000467211, h = 0.0000229736$ for $\lambda_1 = 1, \lambda_2,$ and $0.4\lambda_2$

TABLE VIII

RMI AND AEQL VALUES FOR INDICATED PERFORMANCE OF CHARTS

Control chart		EWMA	DEWMA	
λ_2	λ_1	$\lambda_1 = 1$	$\lambda_1 = \lambda_2$	$\lambda_1 = 0.4\lambda_2$
0.05	RMI	1.269	0.460	0.000
	AEQL	0.065	0.045	0.037
0.10	RMI	0.667	0.317	0.000
	AEQL	0.066	0.053	0.043

[14] S. Crowder, "Average Run Lengths of Exponentially Weighted Moving Average Control Charts," *Journal of Quality Technology*, vol. 19, no. 3, pp. 161-164, 1987.

[15] L.N. Vanbrackle III and M.R. Reynolds Jr., "EWMA and CUSUM Control Charts in the Presence of Correlation," *Communications in Statistics - Simulation and Computation*, vol. 26, no. 3, pp. 979-1008, 1997.

[16] S. Phanyaem, "Average Run Lengths of Cumulative Sum Control Charts for SARMA(1,1)L Models," *Thailand Statistician*, vol. 15, no. 2, pp. 184-195, 2017.

[17] K. Karoon, Y. Areepong and S. Sukparungsee, "Trend Autoregressive Model Exact Run Length Evaluation on a Two-Sided Extended EWMA Chart," *Computer Systems Science and Engineering*, vol. 44, no. 2, pp. 1143-1160, 2023.

[18] K. Karoon, Y. Areepong and S. Sukparungsee, "Exact Run Length Evaluation on Extended EWMA Control Chart for Seasonal Autoregressive Process," *Engineering Letters*, vol. 30, no. 4, pp. 1377-1390, 2022.

[19] P. Phanthuna, Y. Areepong and S. Sukparungsee, "Detection Capability of the Modified EWMA Chart for the Trend Stationary AR(1) Model," *Thailand Statistician*, vol. 19, no. 1, pp. 69-80, 2021.

[20] K. Karoon and Y. Areepong, "Improving Sensitivity of the DEWMA Chart with Exact ARL Solution under the Trend AR(p) Model and its Applications," *Emerging Science Journal*, vol. 7, no. 6, pp. 1875-1891,

2023.

[21] Y. Areepong and K. Karoon, "Explicit ARL Formulas on DEWMA Chart for Seasonal Autoregressive Model with Application in Air Pollution," *IAENG International Journal of Computer Science*, vol. 50, no. 4, pp. 1202-1220, 2023.

[22] P. Phanthuna, Y. Areepong and S. Sukparungsee, "Performance Measurement of a DMEWMA Control Chart on an AR(p) Model with Exponential White Noise," *Applied Science and Engineering Progress*, vol. 17, no. 4, pp. 7088, 2024.

[23] M. Sofonea, W. Han and M. Shillor, *Analysis and Approximation of Contact Problems with Adhesion or Damage*, Chapman and Hall/CRC, Academic Press, New York, 2005.

[24] K. Karoon and Y. Areepong, "Modification of ARL for Detecting Changes on the Double EWMA Chart in Time Series Data with the Autoregressive Model," *Connection Science*, vol. 35, no. 1, pp. 2219040, 2023.

[25] V. Alevizakos, K. Chatterjee and C. Koukouvinos, "The Triple Exponentially Weighted Moving Average Control Chart," *Quality Technology and Quantitative Management*, vol. 18, no. 3, pp. 326-354, 2021.